Pergamon

Spectrochimica Acta, Vol. 50B, No. 2, pp. 179–196, 1995

0584–8547/95 $9.50 + .00

0584–8547(94)00117–0

Monte Carlo simulation of an analytical glow discharge: motion of electrons, ions and fast neutrals in the cathode dark space

ANNEMIE BOGAERTS*, MARK VAN STRAATEN and RENAAT GIJBELS
Department of Chemistry, University of Antwerp, Universiteitsplein 1, B–2610 Wilrijk-Antwerp, Belgium

(*Received* 27 *May* 1994; *accepted* 18 *August* 1994)

Abstract—To understand and to optimize the results obtained with analytical techniques which use a glow discharge as an atomization, excitation or ionization source, an insight in the fundamental processes of the glow discharge is necessary. This insight can be obtained by theoretical modeling studies. In this work, a Monte Carlo simulation is described for the electrons, ions and fast neutrals in the cathode dark space, and the results are compared with results of a kinetic model. The effect of anisotropic angular scattering and elastic collisions on the plasma properties and on the sputtering process is illustrated.

1. INTRODUCTION

A GLOW discharge is a plasma, containing approximately equal concentrations of positive and negative charges plus large numbers of neutral species. In its simplest form, the glow discharge consists of two electrodes inserted into a low pressure inert gas environment (10–1000 Pa). A voltage of 200–2000 V is applied between the electrodes and causes electrical breakdown of the gas, thereby producing positive ions and electrons. The positive ions are accelerated towards the cathode by the strong electric field in front of it, causing secondary electron emission from the cathode. The electrons are in turn accelerated away from the cathode, and acquire energies sufficiently high for ionization and excitation. The excitation processes (and the subsequent desexcitations) are responsible for the characteristic light of the "glow" discharge. The ionization processes create new ions and electrons, essential to maintain the glow discharge.

Glow discharges are used for deposition and etching of thin films such as for microelectronics applications [1] and as an analytical spectroscopic source for elemental analysis [2–9]. These applications are based on the phenomenon of sputtering in a glow discharge. In addition to secondary electron emission from the cathode, the ion bombardment causes also the sputtering of cathode material. This sputtered material consists predominantly of free atoms, and that makes the glow discharge useful for element analysis (GDMS, GD–OES, GD–AAS). The most important analytical applications are found in bulk analysis and depth profiling of conducting materials, but semi-conductors, non-conductors, thin films and solutions can in principle be analysed as well.

For good analytical practice, an understanding of the fundamental processes occurring in a glow discharge is desirable. This apprehension can theoretically be acquired by modelling studies and experimentally by plasma diagnostical measurements. Glow discharges have been modelled many times for regimes used in the field of plasma deposition and etching [10–23], but analytical glow discharges have not so extensively been studied in that way. The external parameters of the former type of glow discharges (pressure, voltage, current, discharge geometry . . .) may be different, but the physical properties are essentially comparable.

Generally, there are three types of modelling. A fluid model [10–14] assumes that

* Author to whom correspondence should be addressed.

all species in the discharge are in hydrodynamic equilibrium. The species are treated in a group as a continuum. The governing equations are the continuity equations (fluxes and densities of the species) and the Poisson equation for the description of the electric field. In a kinetic model [15–18], the plasma species are considered as fluxes ("beams of particles") described by the Boltzmann transport equations, again combined with the Poisson equation for the electric field. Finally, a Monte Carlo simulation [19–23] describes the different plasma particles separately on a statistical basis. This is probably the most accurate method, but it requires considerable computer time. The fluid model is the simplest but also the most approximate one, considering that the electrons are not in equilibrium with the strong electric field.

The glow discharge can be subdivided in several zones between anode and cathode, but in the case of an analytical glow discharge only two zones are usually considered: the cathode dark space (CDS) which is a thin, relatively dark layer next to the cathode surface, characterized by a high electric field, and the negative glow (NG), the most luminous region due to many excitation (and also ionization) collisions. The latter is a quasi-equipotential region and occupies nearly the whole interelectrode space. The CDS is the most important region of the glow discharge. A glow discharge can be maintained without NG and the other zones, but not without the CDS.

In this work, a Monte Carlo simulation is described for electrons, ions and fast neutrals arising from charge exchange collisions, in the CDS. A comparison is made with a kinetic ("Boltzmann") model for the electrons, ions and fast neutrals.

2. DESCRIPTION OF THE MODEL

A. Model assumptions

The discharge we want to model has a cylindrical geometry with a flat cathode, hence the model calculation in three dimensions is generally reduced to only two dimensions: axial and radial. However in this model, no radial effects (diffusion to the walls . . .) will be considered and the electric field is assumed to be only axial. Therefore, the computation applies to a discharge between two infinitely wide parallel plates (respectively the cathode and the interface between CDS and NG), and the calculations are only one-dimensional. Nevertheless, angular deflections by collisions are already taken into account, so that the species do not only move in a direction perpendicular to the cathode, but also in other directions. Hence, the model is one-dimensional with already the incorporation of three-dimensional angular scattering. In future work, full three-dimensional calculations will be done.

The discharge gas (argon) is assumed to be at room temperature and only weakly ionized. The plasma consists of four species: neutral ground state argon atoms at rest and uniformly distributed throughout the discharge (Ar^0), electrons (e^-), singly charged positive argon ions (Ar^+) and fast argon atoms (Ar^0_f). The neutral (slow) argon atom density is much larger than the densities of electrons, argon ions and fast argon atoms, so that only collisions of electrons, ions and fast atoms with these slow argon atoms are incorporated. Collisions of electrons, ions and fast neutrals with each other are neglected. The collisions taken into account are excitation, ionization and elastic collisions between electrons and argon atoms, charge exchange and elastic collisions between argon ions and atoms, and elastic collisions of fast argon atoms with slow argon atoms. Secondary electron emission at the cathode is only due to ion bombardment, fast atom bombardment at the cathode causes very little secondary electron emission in the energy range considered here [1] and can hence be neglected.

B. The Monte Carlo simulation

The Monte Carlo procedure simulates a large number of particles (electrons, ions and fast neutrals). The trajectory of the particles is described by Newton's laws:

$$x = x_0 + v_{x_0}\Delta t + \frac{q}{2m}\mathscr{E}_{x_0}(\Delta t)^2$$

$$r = r_0 + v_{r_0}\Delta t \tag{1}$$

$$v_x = v_{x_0} + \frac{q}{m}\mathscr{E}_{x_0}\Delta t$$

$$v_r = v_{r_0}$$

where x_0 and r_0 are, respectively, the initial axial and radial positions of the particle, and x and r are the axial and radial positions after the particle has travelled a distance Δs; in a similar way we call v_{x0} and v_{r0} the initial velocities of the particle in the axial and the radial directions, and v_x and v_r the velocities in the axial and radial directions after the distance Δs. $\mathscr{E}_{x0}$ is the electric field at position x_0, Δt is the timestep corresponding to the distance Δs, and q and m are, respectively, the charge and mass of the particle.

The electric field is assumed to vary linearly with the distance from the cathode [24]:

$$\mathscr{E}_{x_0} = \frac{-2V_c}{d_c}\left(1 - \frac{x_0}{d_c}\right) \tag{2}$$

where V_c is the voltage applied to the cathode and d_c is the length of the CDS.

The probability of a collision event and the new energy and direction of a particle after a collision are determined by a sequence of random numbers.

We calculate the probability, P, of a collision in the distance Δs by:

$$P = 1 - \exp(-n\sigma_{tot}(E)\Delta s) \tag{3}$$

where n is the slow argon atom density and $\sigma_{tot}(E)$ is the total collision cross section of the particle with energy E, with an argon atom. This equation is only valid when Δs is small enough so that the energy (and hence $\sigma_{tot}(E)$) can be regarded constant over this distance.

A random number between 0 and 1 is generated and compared with P. If the random number is larger than P, no collision has occurred and the particle follows its way as if nothing happened. If the random number is smaller than P, a collision has occurred. To determine the nature of the collision, the total cross section $\sigma_{tot}(E)$ is split up into its component cross sections for all the possible collision processes of that particle, and the fractional probability of a certain kind of collision is computed:

* for electrons:

$$\sigma_{e,tot}(E) = \sigma_{ioniz}(E) + \sigma_{exc}(E) + \sigma_{e,ela}(E)$$

$$P_{ion} = \frac{\sigma_{ioniz}(E)}{\sigma_{e,tot}(E)} \tag{4}$$

$$P_{exc} = \frac{\sigma_{exc}(E)}{\sigma_{e,tot}(E)}$$

$$P_{e,ela} = \frac{\sigma_{e,ela}(E)}{\sigma_{e,tot}(E)}$$

* for ions:

$$\sigma_{i,tot}(E) = \sigma_{charge}(E) + \sigma_{i,ela}(E)$$

$$P_{charge} = \frac{\sigma_{charge}(E)}{\sigma_{i,tot}(E)} \tag{5}$$

$$P_{i,ela} = \frac{\sigma_{i,ela}(E)}{\sigma_{i,tot}(E)}$$

* for neutrals:

$$\sigma_{n,tot}(E) = \sigma_{n,ela}(E)$$
$$P_{n,ela} = 1 \tag{6}$$

where P_{ioniz}, P_{exc} and $P_{e,ela}$ are respectively the fractional probability of an ionization, excitation and elastic collision for an electron; P_{charge} and $P_{i,ela}$ are respectively the fractional probability of a charge exchange and elastic collision for an ion, and $P_{n,ela}$ is the fractional probability of an elastic collision for a fast neutral (which is of course equal to one).

The sum of the fractional probabilities for each kind of particle is equal to unity and the interval [0, 1] is divided into segments of lengths corresponding to these fractional probabilities. A second random number between 0 and 1 is generated and the segment into which this random number falls, determines the type of collision that has occurred. The new energy and direction after the collision are determined by other random numbers (see further). After the collision, the particle follows its way during the next timestep and the procedure is repeated.

C. Simulation of the electrons

The electrons start at the cathode, created by secondary electron emission due to ion bombardment. The energy of the electrons emitted by the cathode has a distribution between 0 and 6 eV with a maximum of 4 eV [1]. Here the electron energy distribution is approximated by a single value of 4 eV. This choice is justified because it has no influence on the final results, the reason being the rapid acceleration of the electrons in the CDS [25]. The angular distribution is assumed to be isotropic between 0 and $\pi/2$ [19]. The electrons are followed on their way towards the interface between CDS and NG. The method for determining the occurrence and the nature of a collision has already been explained. The new energy and direction after a collision depend on the type of collision:

(i) Excitation: the new energy E is given by:

$$E = E_0 - E_{exc} \tag{7}$$

where E_{exc} is the excitation threshold (taken as 12 eV) and E_0 is the electron energy before collision.

(ii) Ionization: the total energy before collision is divided between the primary and the secondary electron using a random number (RN). The energy of the primary electron (E_{prim}) after the collision is defined by:

$$RN = \frac{\int_0^{E_{prim}} \sigma_{ioniz}(E_0,\epsilon)d\epsilon}{\sigma_{ioniz}(E_0)} \tag{8}$$

where $\sigma_{ioniz}(E_0,\epsilon)$ and $\sigma_{ioniz}(E_0)$ are, respectively, the differential ionization cross section and the total ionization cross section, E_0 is the energy before collision and ϵ is the possible energy of the primary electron. The energy of the secondary electron after the collision is then:

$$E_{sec} = E_0 - E_{ioniz} - E_{prim} \tag{9}$$

where E_{ioniz} is the ionization threshold (taken as 15.76 eV).

(iii) Elastic collision: the kinetic energy of an electron which has undergone an elastic collision with an Ar atom is given by [26]:

$$E = E_0 \left(1 - 2\frac{m_e}{m_{at}}(1 - \cos\chi)\right) \tag{10}$$

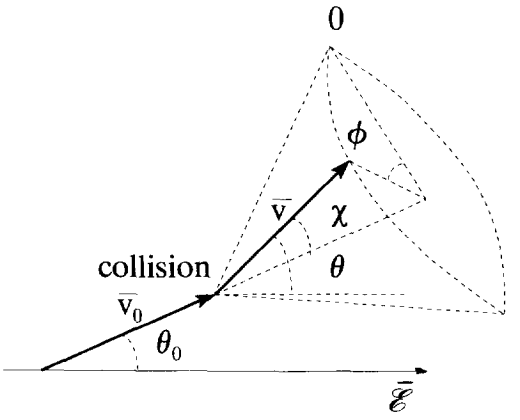

Fig. 1. Definition of the different angles used in the calculations: θ_0 and θ are the angles with respect to the electric field before and after collision, respectively. χ is the scattering angle and ϕ is the azimuthal angle. v_0 and v are the velocities before and after collision, respectively. $\mathscr{E}$ is the direction of the electric field, i.e. the axial direction.

which is deduced from the hard-sphere model. χ is the scattering angle of the electron after collision (see further).

The new direction after each kind of collision is determined by anisotropic scattering [15]. The scattering angle χ and the azimuthal angle ϕ are defined by two random numbers:

$$RN = \frac{2\pi}{\sigma(E_0)} \int_0^{\chi} \sigma(E_0,\chi')\sin\chi' d\chi'$$

$$\phi = 2\pi RN \tag{11}$$

where $\sigma(E_0)$ is the total elastic cross section and $\sigma(E_0,\chi')$ is the angular differential elastic cross section (see further).

The new direction after collision can then be deduced from [19, 21]:

$$\cos\theta = \cos\theta_0\cos\chi + \sin\theta_0\sin\chi\cos\phi \tag{12}$$

where θ_0 and θ are the angles with respect to the axial direction, before and after the collision, respectively. In Fig. 1 the definition of the different angles used above is clarified.

After a collision, the electron follows its way, and the procedure is repeated. In the case of ionization, the primary electron is followed first and the secondary electron is stored. The electron is followed until it reaches the interface between CDS and NG. Then the stored secondary electrons are treated in the same way. When all the secondary electrons have arrived at the interface, the next electron starts at the cathode. For statistical reasons, we have to follow a sufficiently large number of electrons in this way (e.g. 10^5).

D. Simulation of the ions

In the case of an ionizing collision, not only a secondary electron is formed, but also an ion. The transport of these ions, together with the ones starting at the interface between CDS and NG, is also modelled by a Monte Carlo simulation, and this independently from the simulation of the electrons. Electron–ion collisions are not taken into account due to the relatively low density of both compared to the slow argon atom density, and hence the motion of ions and electrons can be assumed to be independent of each other [22]. It is very important that the relative proportion of the number of ions formed at each position in the CDS and the number of ions which

diffuse into the CDS from the NG is correct [22]. The number of ions formed at each position in the CDS is taken from the ionization rates at each position, calculated in the electron simulation. The number of ions which diffuse into the CDS is taken from the ion current at the CDS–NG interface, which is obtained from the total current (independent of distance) and the electron current at the interface calculated in the electron simulation ($j_{tot} = j_i - j_e$). The proportion of the number of ions which diffuse from the NG into the CDS, to the total number of ions formed in the CDS, has a value of about 14–15. Relatively few ions are hence formed in the CDS.

The ions are followed from the CDS–NG interface towards the cathode in the same way as the electrons are followed from the cathode towards the interface. The new energy and direction after collision depend upon the type of collision:

(i) Charge exchange collision: when a fast argon ion collides with a slow argon atom, an electron is transferred from the atom to the ion without any change in kinetic energy of the species, and hence a fast argon atom and a slow argon ion arise.

$$Ar_f^+ + Ar_s^0 \rightarrow Ar_f^0 + Ar_s^+ \tag{13}$$

The new ion starts at rest, so its energy after collision is 0 eV and its new direction is therefore taken parallel to the electric field.

(ii) Elastic collision: data from differential cross sections (like for the electrons) are not generally available, so another method is applied to find the scattering angle. The complete description of this strategy can be found in a work of WRONSKI [21]. To avoid the long numerical calculation, we have used an empirical formula which describes the new scattering angle in terms of the energy of the ion and the impact parameter [27]:

$$\sin^2\left(\frac{\chi_{COM}}{2}\right) = \left(1 + \frac{p^2\epsilon^{2/n}}{(K_n^2\beta_n)^{1/n}}\right)^{-n} \tag{14}$$

where p is the reduced impact parameter, ϵ is the reduced energy of the ion, n is the parameter of inverse power potential, and β_n and K_n are analytical functions of n, p and ϵ. The complete description of this formula can be found in [27]. The determination of the impact parameter out of the energy is described in [21]. Conversion of the scattering angle in the centre-of-mass frame of reference, χ_{COM}, to the scattering angle of the ion, $\chi_{lab,ion}$, and of the atom, $\chi_{lab,at}$, in the laboratory frame of reference is carried out in the following way [21, 26]:

$$\tan\chi_{lab,ion} = \frac{\sin\chi_{COM}}{\left(\frac{m_{ion}}{m_{at}}\right) + \cos\chi_{COM}} = \frac{\sin\chi_{COM}}{1 + \cos\chi_{COM}}$$

$$\Rightarrow \chi_{lab,ion} = \frac{\chi_{COM}}{2} \tag{15}$$

$$\chi_{lab,at} = \frac{1}{2}(\pi - \chi_{COM}) = \frac{\pi}{2} - \chi_{lab,ion}$$

where m_{ion} and m_{at} are the masses of the ion and the atom, respectively.

The azimuthal angle is defined in the same way as for the electrons (Eqn (11)), and the new angle after collision with respect to the axial direction can then be calculated by equation (12). The new energy of the ion after an elastic collision (E_{ion}) can be found by [26]:

$$E_{ion} = E_{0,ion}\left(1 - \frac{4\mu^2}{m_{at}m_{ion}}\cos^2\chi_{at,lab}\right) = E_{0,ion}(1 - \cos^2\chi_{at,lab}) \tag{16}$$

where $E_{0,ion}$ is the energy of the ion before the collision, and μ is the reduced mass of the collision partners:

$$\mu = \frac{m_{at} m_{ion}}{m_{at} + m_{ion}} \tag{17}$$

In this way, all the ions are followed, one after the other.

E. Simulation of the fast atoms

When the ions have undergone a charge exchange collision or an elastic collision, a fast neutral arises. In the case of a charge exchange collision, this fast neutral has the energy and direction of the ion before the collision, because only an electron is transferred and no kinetic energy is exchanged. In the case of an elastic collision, the new direction of the fast neutral is calculated in the same way as for the ions. The scattering angle ($\chi_{lab,at}$) is given by equation (15). The azimuthal angle is calculated by Eqn (11) and finally the new angle after collision with respect to the axial direction is defined by Eqn (12). The new energy of the fast atom after collision (E_{at}) is defined by the law of conservation of energy and is thus given by:

$$E_{at} = E_{0,ion} - E_{ion} \tag{18}$$

where $E_{0,ion}$ and E_{ion} are the energy of the ion before and after the elastic collision, respectively.

During the modelling of the ions, the fast neutrals formed by charge exchange and elastic collisions are stored and are afterwards put in the Monte Carlo simulation of the fast neutrals. These fast neutrals are followed in the same way as the ions and the electrons, except that they do not experience the force of an electric field. The only kind of collision taken into account is the elastic collision. This elastic collision can be considered nearly identical to the elastic collision of the ions [28, 29], hence the method of calculation of the new direction and energy is identical. By these elastic collisions, also new fast neutrals are formed and their energy and direction are calculated in the same way as for ion-atom elastic collisions.

The fast neutrals are followed until they reach the cathode or the interface between CDS and NG, or until their energy is less than 0.05 eV. Indeed, if the energy is less than this value (~kT, the thermal energy), the neutrals can be considered thermalized and be put in the large "slow" atom group.

F. Collision cross sections

The cross sections for the electron collisions considered here are shown in Fig. 2 (numbers 1–4). We have combined all the various excitation processes into one composite excitation process with a threshold energy of 12 eV. The composite excitation cross section is taken from ref. [30]. The ionization cross sections (both differential and total) are from ref. [17]. The elastic cross section is obtained by fitting the experimental results given in ref. [31] (lower energies) and [32] (higher energies). The differential angular cross section, required for the calculation of the scattering angle in the case of anisotropic scattering, is taken from ref. [15]. Substituting the analytical expression of $\sigma(E_0,\chi)/\sigma(E_0)$ found there into the integral given in Eqn (11), and solving it analytically, yields:

$$\chi = 2 \arcsin \sqrt{\frac{\exp[RN \ln(1 + E_0)] - 1}{E_0}} \tag{19}$$

The collision cross sections for the different types of ion collisions are also plotted in Fig. 2 (numbers 5–7). The cross section for charge exchange is taken from [29]. The method of calculating the elastic cross section is described in [21]. Often elastic collisions of ions are neglected with respect to charge exchange collisions [18, 25, 33],

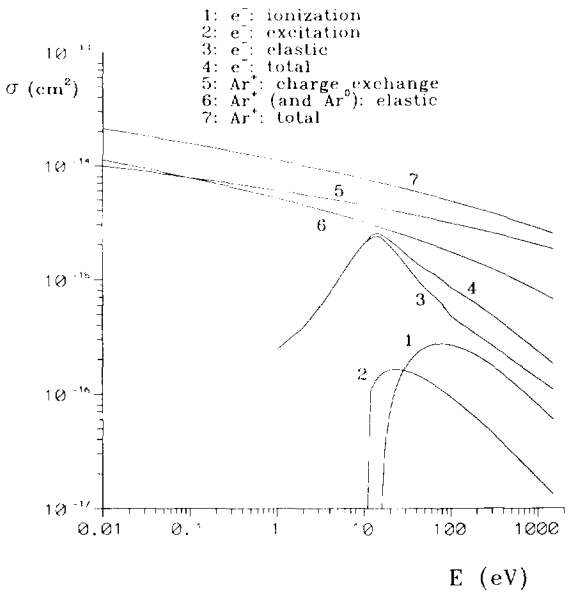

Fig. 2. Cross sections for the different collision processes in an argon glow discharge, included in the model.

but Fig. 2 shows that this is not really allowed. The cross section for fast neutral elastic collisions is assumed to be the same as that for ion elastic collisions [28, 29].

3. Results and Discussion

In the present work, an argon glow discharge is considered. The discharge conditions used in the calculations (750 mtorr; 5.29 mA/cm^2 and 962 V) are experimentally obtained by mounting a molybdenum cathode in the standard discharge cell of a VG 9000 glow discharge mass spectrometer for analysing flat samples [34]. The present model is not self-consistent. We considered a linearly decreasing field in the CDS and assumed that the length of the CDS was 0.15 cm, a value which we have calculated before [25, 33], based on a kinetic model such as described by ABRIL [18]. The secondary electron emission coefficient for Mo is taken to be 0.12 [1]. This coefficient is not exactly known. It depends on the ion energies, the condition of the cathode surface, etc. However, in ref. [1] is shown that these parameters have no significant influence on the emission coefficient for Ar ion bombardment on a Mo sample. Moreover, the obtained results should be considered only semi-quantitative, and changing the value of the secondary electron emission coefficient changes only the value of the currents but has no effect on the characteristic shape of the results [25].

3.1. *Results of the Monte Carlo simulations*

A. Distribution functions for electrons, ions and fast neutrals. Figure 3a shows the spatial variations of the energy distribution function, $n(x,E)dE$, of the electrons in the CDS. Electrons are emitted by the cathode ($x = 0$ cm) with an energy of 4 eV. In the CDS, they are accelerated by the electric field and gain energy on their way to the CDS–NG interface. When they reach an energy of 12 eV and more, they can cause excitation of argon atoms and lose an energy of 12 eV. When reaching an energy of about 16 eV and more, they can ionize neutral gas atoms and produce new electrons with lower energies. In this way, by moving towards the negative glow, the energy of the electrons increases due to the acceleration in the electric field and at the same time, the energy is spread out over lower energies as a result of collisions. At the end of the CDS, the major fraction of the electrons still has not participated

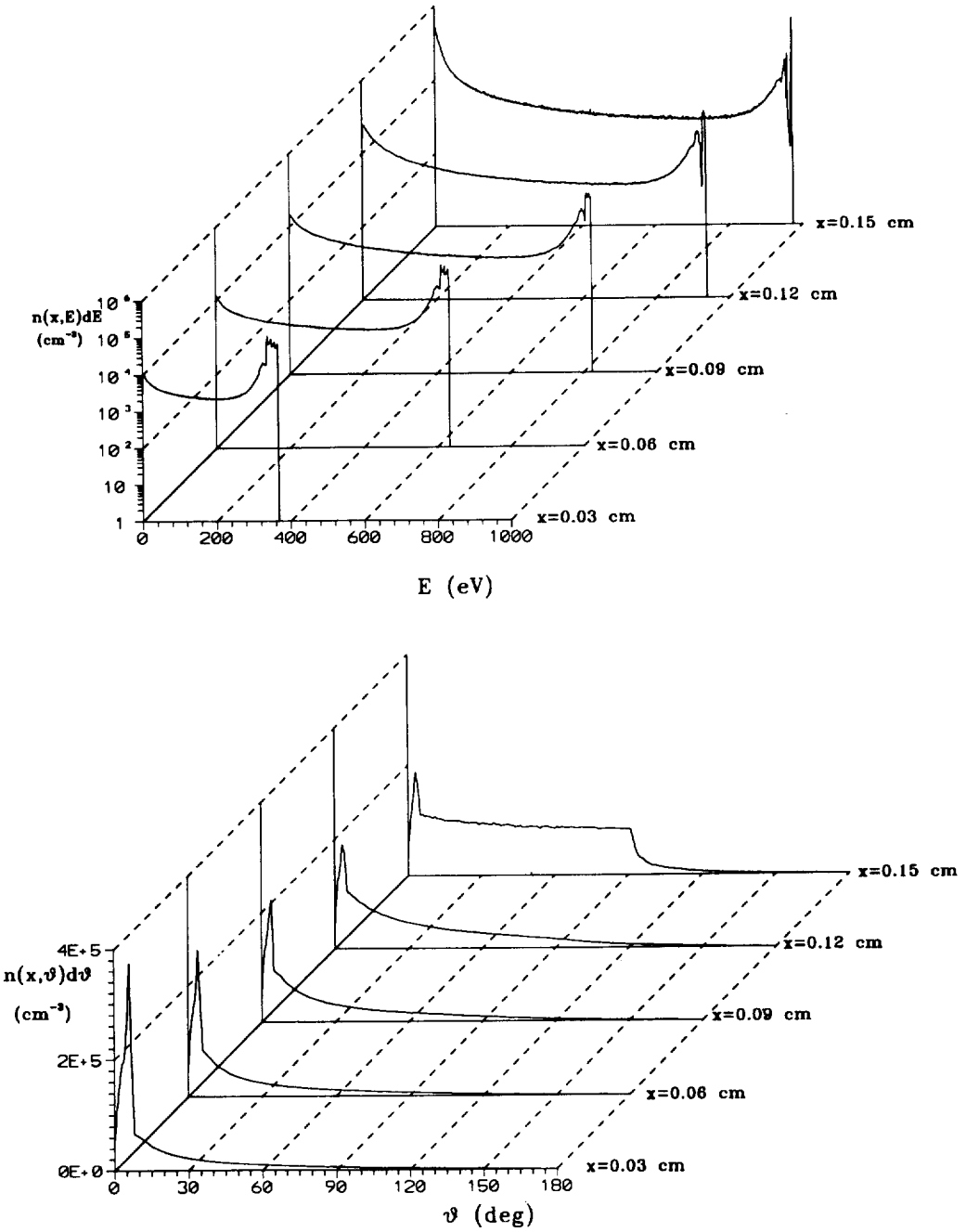

Fig. 3. Energy distribution (a) and angular distribution (b) of the electrons in the CDS at different positions from the cathode.

in any collision process in the CDS, as indicated by the large peak at the maximum attainable energy (eV_{disch}) in the Figure.

In Fig. 3b the spatial variations of the electron angular distribution function, $n(x,\theta)d\theta$, in the CDS is presented. The angular distribution has a maximum value at angles of about 5°. The reason for this is that scattering is most probable for angles near 5°. After this maximum, the angular distribution first drops off very sharply and then it decreases further for increasing angles. When the electrons continue their way to the NG, larger angles become slightly more abundant, and close to the NG the electrons move in approximately all directions between 0° and 90° with the axis of the system. The near absence of electrons scattered at higher angles near the CDS–NG

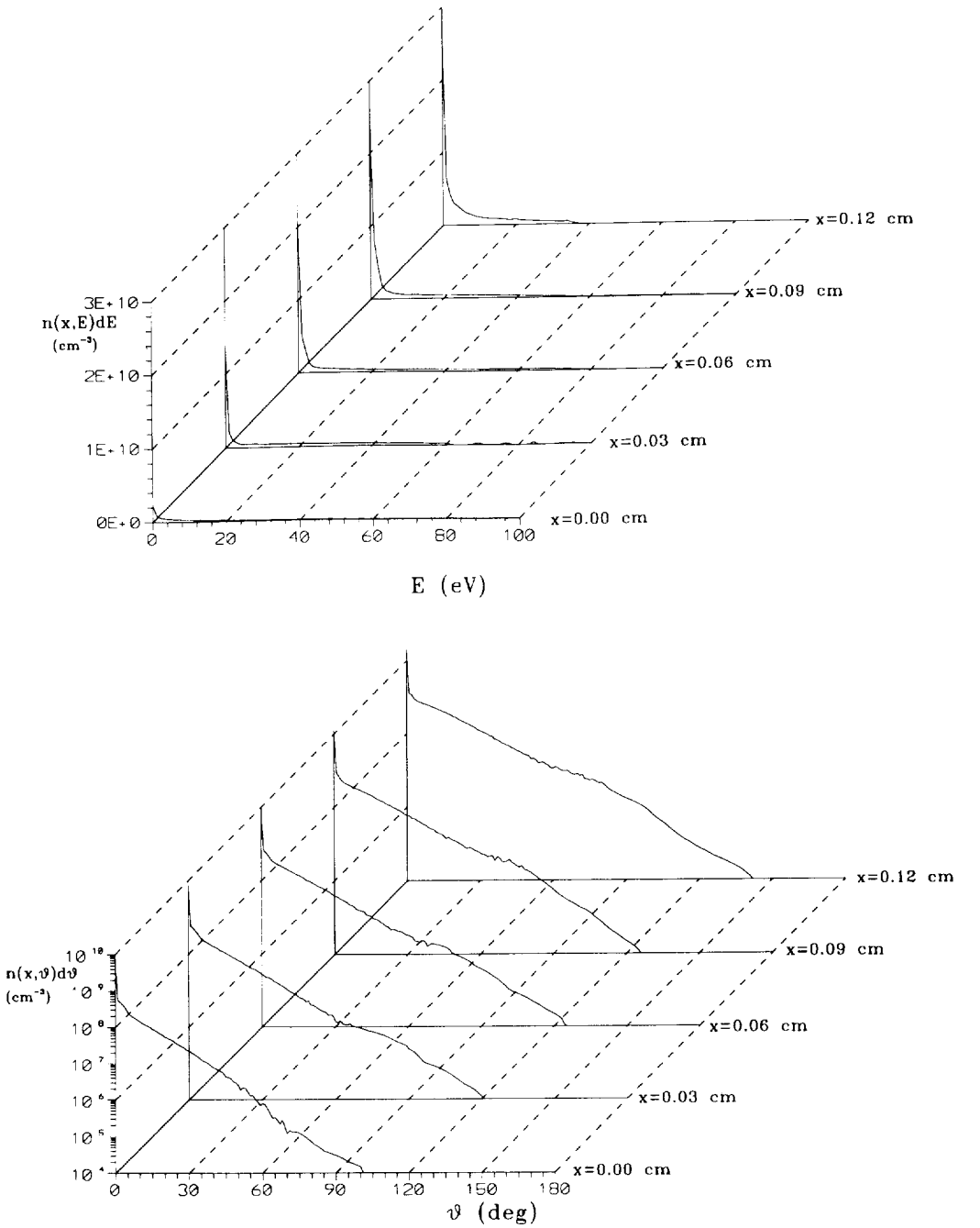

Fig. 4. Energy distribution (a) and angular distribution (b) of the Ar ions in the CDS at different positions from the cathode.

interface is due to the artificial absorbing effect of the interface in this model. When the electrons arrive at the NG, the calculation stops. There is no possibility for the electrons to be scattered in the NG and return back into the CDS at an angle of more than 90°. Hence this result is an artefact of the calculations and does not necessarily reflect the real situation.

The spatial variation of the energy distribution function of the ions, $n(x,E)dE$, in the CDS is given in Fig. 4a. The ions start at the interface between CDS and NG (behind the Figure, at $x = 0.15$ cm) with zero energy and move towards the cathode ($x = 0$ cm), thereby gaining energy from the electric field and losing energy by collisions. Contrary to the electrons (Fig. 3a), there is no peak corresponding to ions

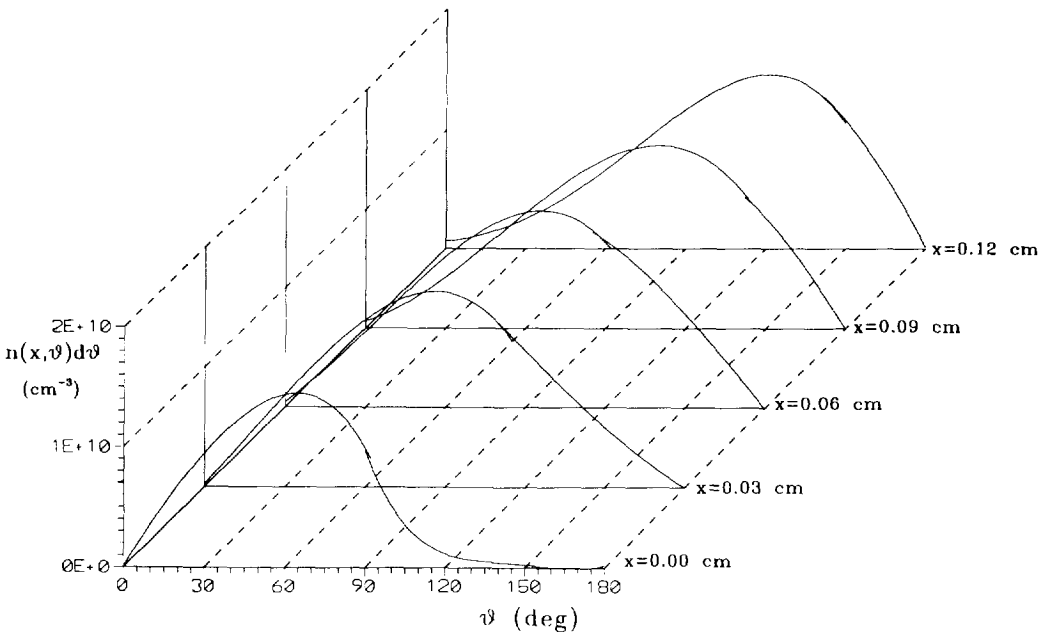

Fig. 5. Angular distribution of the Ar fast neutrals in the CDS at different positions from the cathode.

which did not suffer any collision. Instead, the energy distribution peaks at low energy and decreases monotonically with increasing energy. We conclude that the collision processes of the ions (charge exchange and elastic collisions) are very effective for reducing and spreading out the ion energy. It should also be noted that the energy axis in the figure is truncated at a value lower than the energy corresponding to the full discharge potential of 962 V.

Figure 4b illustrates the development of the angular distribution of the ions, $n(x,\theta)d\theta$, in the CDS. The zero angle is by far the most probable one (i.e. more than a factor of ten; note the logarithmic scale). The reason for this is that charge exchange collisions are more frequent than elastic collisions, and each time the ion undergoes a charge exchange collision, the ion starts again from rest in the direction parallel to the electric field, so most of the ions move completely forward. At larger angles, the distribution decays continuously. Angles of more than 90° are very rare, because the ions are so strongly directed towards the cathode by the electric field.

The energy distribution of the fast neutrals in the CDS qualitatively resembles that of the ions (i.e. monotonically decreasing with increasing energies), which is obvious because the fast neutrals are formed directly from the ions. The energy distribution is however strongly shifted to lower energies compared to the distribution of the ions, because the neutrals cannot gain energy from the electric field; they can only lose energy by elastic collisions. Hence, 85% of the "fast" neutrals has nearly thermal energies at the cathode and about 98% of them has energies less than 4 eV.

Figure 5 shows the angular distribution of the fast neutrals, $n(x,\theta)d\theta$, in the CDS. Because fast neutrals undergo many scattering collisions and are not directed to the cathode by the electric field, as is the case for the ions, they have a wider angular distribution. The most probable angle of motion is found between 60° and 120°, because of the larger probability of scattering at these angles. Close to the cathode, most of the fast neutrals move at angles lower than 90° (that means: directed towards the cathode), but further away from the cathode and especially near the NG, relatively more fast neutrals have angles larger than 90°, indicating that they are directed away from the cathode.

B. Other calculated characteristic quantities for electrons, ions and fast neutrals. The calculated mean energies, $<E>$, of the electrons, ions and fast neutrals are plotted in

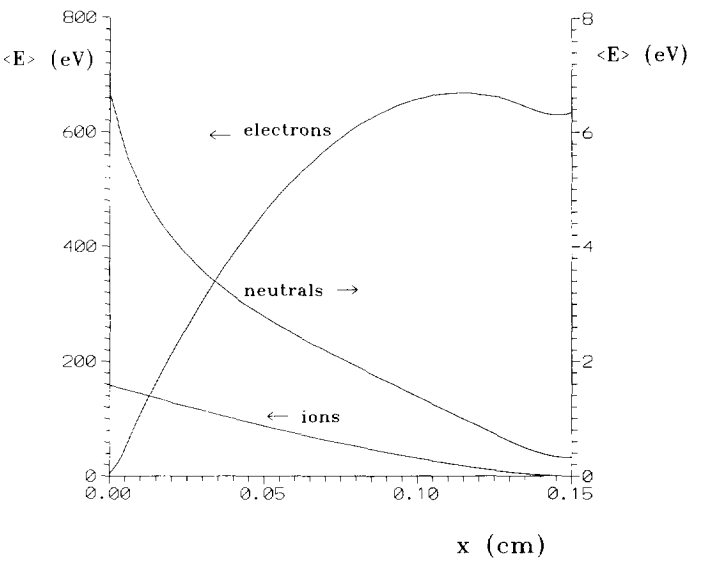

Fig. 6. Spatial dependence of the mean energies of the electrons, Ar ions and fast neutrals in the CDS.

Fig. 6. The energy of the electrons increases towards the negative glow, reaches a maximum of nearly 700 eV and slighty decreases again. This means that closer to the cathode, where the electric field is very high, the energy gain due to the electric field exceeds the energy loss by the collisions, but near the CDS–NG interface the situation is slightly reversed, because the electric field is much lower there. We clearly see that the electrons are not in equilibrium with the electric field. The mean energy of the ions gradually increases towards the cathode, reaching a value of about 160 eV, but it is always much lower than the mean energy of the electrons, due to the more efficient and more frequent collisions with argon atoms (see Fig. 2). The fast neutrals have a very low mean energy (lower than 10 eV; see right-hand scale), because they lose considerable energy by elastic collisions but cannot gain energy from the electric field.

The collision efficiencies, q, of the electrons, ions and fast neutrals, i.e. the number of collisions per cm and per particle, are shown in Fig. 7. The elastic collisions of the electrons (3) are more frequent than the ionization (2) and excitation (1) processes due to a higher cross section (illustrated in Fig. 2). About 5 to 20 elastic collisions take place per cm and per electron (this means about 1 to 3 elastic collisions in the CDS per electron), compared to only 3 to 6 electron impact ionization processes and 1 to 3 excitation processes per cm and per electron. The collision efficiency is a combination of Fig. 2 (the cross sections) and Fig. 6 (the mean energy at a given position). When the energy is low, the collision efficiencies are higher because of the higher value of the cross section. Figure 7 also illustrates that ion collisions are very frequent compared to the collision events for electrons. The number of collisions is of the order of 50 to 100 per cm and per ion, and is clearly higher for charge exchange (4) than for elastic collisions (5) due to the higher cross section (cf. Fig. 2). The elastic collisions of the fast neutrals (6) are even more abundant (of the order of 230 per cm and per fast atom) than the collisions of the ions, because of their lower energies.

In Fig. 8 the fluxes, j, are given for the different species in the CDS. The electron flux increases slightly towards the interface between CDS and NG, while the flux of the ions increases in value towards the cathode. The ion flux is negative because the ions move generally in the direction towards the cathode (negative x-axis). The ion flux is one order of magnitude higher than the electron flux indicating that in the CDS most of the electric current is carried by ions. The fast neutral flux (see right-

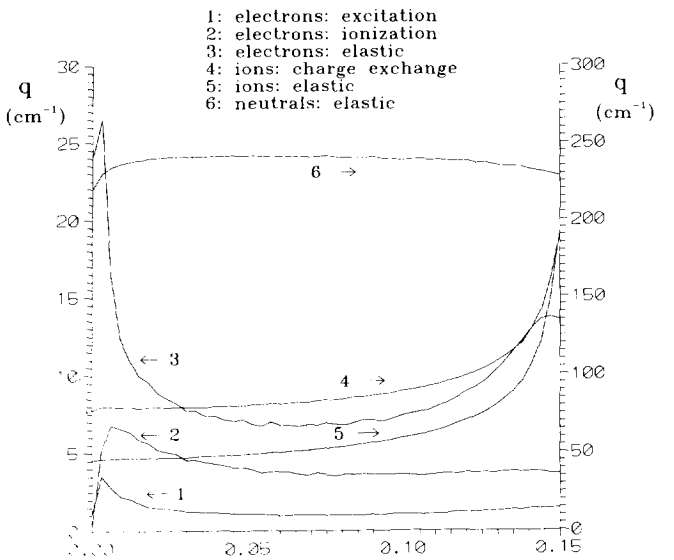

Fig. 7. Spatial dependence of the collision efficiencies of the electrons, Ar ions and fast neutrals in the CDS.

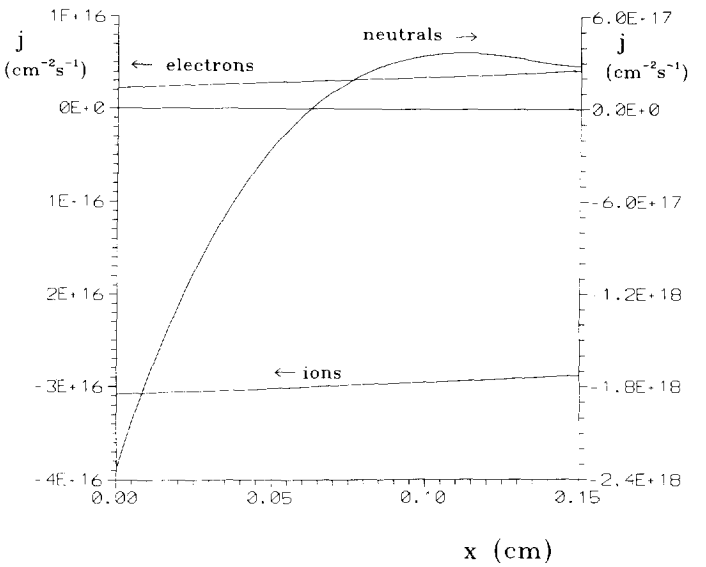

Fig. 8. Spatial dependence of the fluxes of the electrons, Ar ions and fast neutrals in the CDS.

hand scale) is nearly two orders of magnitude higher than the ion flux, due to the very efficient charge exchange and elastic collisions whereby new fast neutrals are created. As was already expected from Fig. 5, the fast neutral flux goes through zero at 0.06 cm from the cathode, indicating that close to the cathode relatively more neutrals are directed towards the cathode and close to the NG, the situation is reversed.

Figure 9 represents the densities, n, of the species in the CDS. The density of the electrons is nearly 10^4 times less than the density of the ions. This means that the CDS is characterized by a strongly positive charge density, as is necessary to provide for the high electric field gradient. The ion density is about constant throughout the CDS, but near the CDS–NG interface it shows a considerable increase. The exact

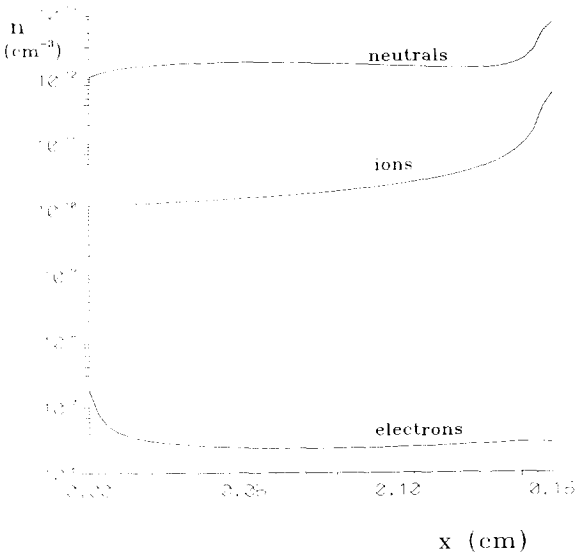

Fig. 9. Spatial dependence of the densities of the electrons, Ar ions and fast neutrals in the CDS.

amount of increase cannot be obtained here, because the model does not include diffusion, and near the NG, diffusion is becoming one of the main transport processes. On the other hand, the nearly constant value obtained closer to the cathode can be considered rather correct. Fast neutral atoms are approximately 2 orders of magnitude more abundant than ions in the CDS.

3.2. *Comparison of the Monte Carlo simulation with a kinetic model; effect of elastic collisions and non-forward scattering.* To determine the effect of non-forward scattering and elastic collisions on particle transport in the CDS, we have compared the present Monte Carlo simulation with a kinetic (Boltzmann) model similar to that described by ABRIL [18]. In such a model both phenomena are usually omitted because of the mathematical complexity which they introduce. We also have carried out the Monte Carlo simulation assuming only forward scattering and neglecting elastic collisions. The results are, as expected, very similar to those of the kinetic model.

The incorporation of elastic collisions and anisotropic scattering results in a lowering of the mean energies of the electrons, ions and fast neutrals. The scattering effect is only 10% for the electrons and ions, since excitation–ionization collisions for the electrons and charge exchange collisions for the ions play a more significant role in determining the energy losses than the elastic collisions. However, the effect is considerable for the fast neutrals, because in the kinetic model no collisions at all were assumed for these species; the mean energy is lowered by a factor of 10 (6 eV at the cathode instead of 60 eV).

The differences in mean energies have only a very little effect on the collision efficiencies. The excitation and ionization efficiencies of the electrons are a bit higher due to the slightly lower energies. The charge exchange efficiency of the ions experiences nearly no effect at all. The effect of scattering of the electrons appears most clearly in the ionization rate (this is: per cm^3 and per sec, for all the electrons together) and hence also in the multiplication rate of the electrons in the CDS. Namely, scattering causes the electrons to stay longer in the CDS and thus to bring about more ionization collisions. More ionization collisions give more secondary electrons and hence a rather higher multiplication rate compared to the case of forward scattering only, as can be seen in Fig. 10. The multiplication factor, $M(x)$, of the electron current reaches a value of 2 in the case when scattering is included, compared to a factor of 1.6 when scattering is not taken into account.

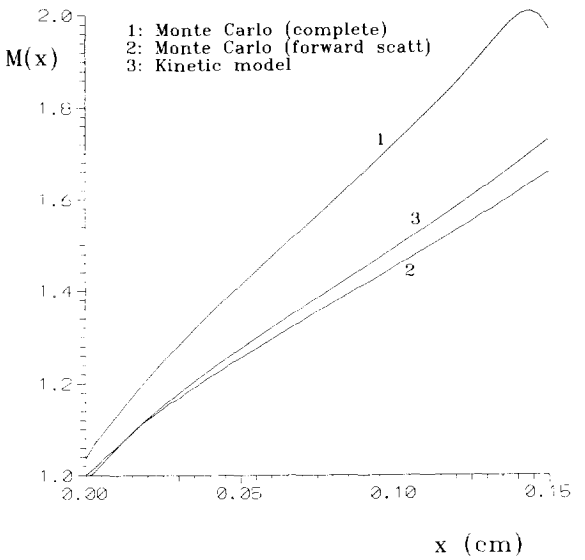

Fig. 10. Comparison of the three models for the spatial dependence of the multiplication rate of the electrons in the CDS.

Due to the more numerous ionization collisions in the Monte Carlo model including scattering, the ion and electron fluxes in the CDS increase by a factor of 15% compared to the results obtained without scattering. The fast neutral flux is changed considerably by the incorporation of elastic scattering. Without any collisions, the fast neutral flux is always negative (always directed towards the cathode) and increases gradually from zero at the CDS–NG interface until a value of -4.10^{17} cm^{-2} s^{-1} at the cathode. The incorporation of elastic scattering causes the creation of more fast neutrals and hence increases the fast neutral flux, compared to the case without scattering. But due to the scattering, the fast neutrals move in all directions, lowering the net flux in one direction; this also results in a change of direction of the net flux at 0.06 cm from the cathode. Comparing Fig. 8 with the results of the model without scattering described above, we see that the net flux at the cathode (in negative direction) is still a factor of 6 higher than when scattering is not included.

The same effect of scattering and elastic collisions is reflected in the densities of the species in the CDS. Lower energies and a larger number of particles (due to more efficient creating collisions) result in higher densities as compared to the values obtained with the models without scattering.

3.3. *Effect of non-forward scattering and elastic collisions on the sputtering process*

Using the flux energy distributions of the gas ions and of the fast neutrals arriving at the cathode, we can calculate the flux of sputtered atoms liberated from the cathode under influence of these bombarding species. We will not include here cathode sputtering by previously sputtered cathode ions ("self sputtering") [35, 36]. The sputtered atoms will first be thermalized and will then diffuse into the plasma. It is possible to calculate a diffusion profile, i.e. a concentration profile of the sputtered atoms throughout the plasma [34, 37, 38]. It is obvious that the sputtering process is strongly related to the number and energy of the bombarding gas ions and fast neutrals. In the previous section we have seen that incorporation of elastic collisions and scattering into the model can have a more or less significant impact on the flux of both neutrals and ions in the CDS, hence these scattering and elastic collisions will also influence the efficiency of the sputtering process. Figure 11 shows the flux energy distributions of the ions and of the fast neutrals at the cathode surface, $J(0,E)dE$, with and without scattering. Due to the scattering, the flux of the fast gas neutrals increases (at the cathode by a factor of 6, as was explained at the end of section 3.2),

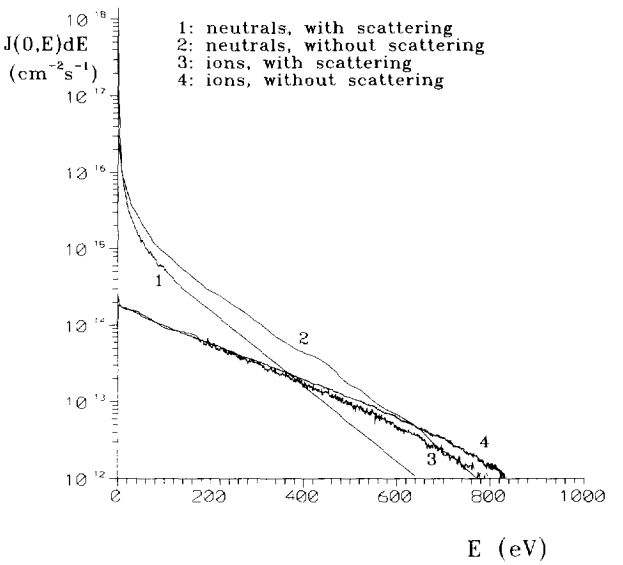

Fig. 11. Flux energy distributions of the Ar ions and fast neutrals at the cathode, calculated with and without scattering.

but in Fig. 11 is shown that this increase applies only for neutrals with low energies ($E < \sim 10$ eV). Moreover, due to the energy losses by elastic scattering, the number of high energy neutrals ($E > \sim 10$ eV) is considerably less than in the case without scattering. Since sputtering is only important when the bombarding particles have energies well above a given threshold energy (which is about 27 eV for Mo), the amount of sputtering due to fast neutrals decreases when elastic scattering is incorporated in the model. We further notice in Fig. 11 that the number of high energy ions is also lowered compared to the case without scattering, but the effect is clearly less pronounced than for the fast neutrals. Hence the calculated amount of sputtering due to ion bombardment also decreases, but to a lower degree than for the fast neutrals. Consequently, the total amount of sputtering decreases by a factor of about 1.5–2, when elastic scattering is incorporated and the relative contribution of ion bombardment to the sputtering process increases slightly, as can be seen by comparing Figs 12a and 12b. Nevertheless, the relative contribution of fast neutrals to the sputtering process is still clearly dominant. Without scattering, the Monte Carlo simulation yields a relative share (summed over all energies) of fast neutrals compared to ions of 80/20, a value comparable to that found using a Boltzmann model [25, 33]; with scattering, this proportion is reduced to 70/30.

4. CONCLUSION

We have used a Monte Carlo model to describe electron, ion and fast atom transport in the CDS of a glow discharge, allowing the incorporation of elastic collisions and anisotropic angular scattering. Typical results obtained by this kind of modelling are the energy and angular distributions, the mean energies, the fluxes and densities of the three kinds of species (electrons, ions and fast neutrals), as well as information on the importance of the collision events in the CDS, all as a function of the distance from the cathode. We have compared this model with a kinetic model and with a Monte Carlo model neglecting scattering and elastic collisions. The latter collision phenomena can have a significant influence on the calculated quantities. First, the energy of all three kinds of species is lowered. Second, because the electrons stay longer in the CDS (due to larger angle scattering), the number of ionization collisions increases, which yields more electrons and ions in the CDS. Third, because new fast neutrals are created by elastic collisions, the number of fast neutrals increases,

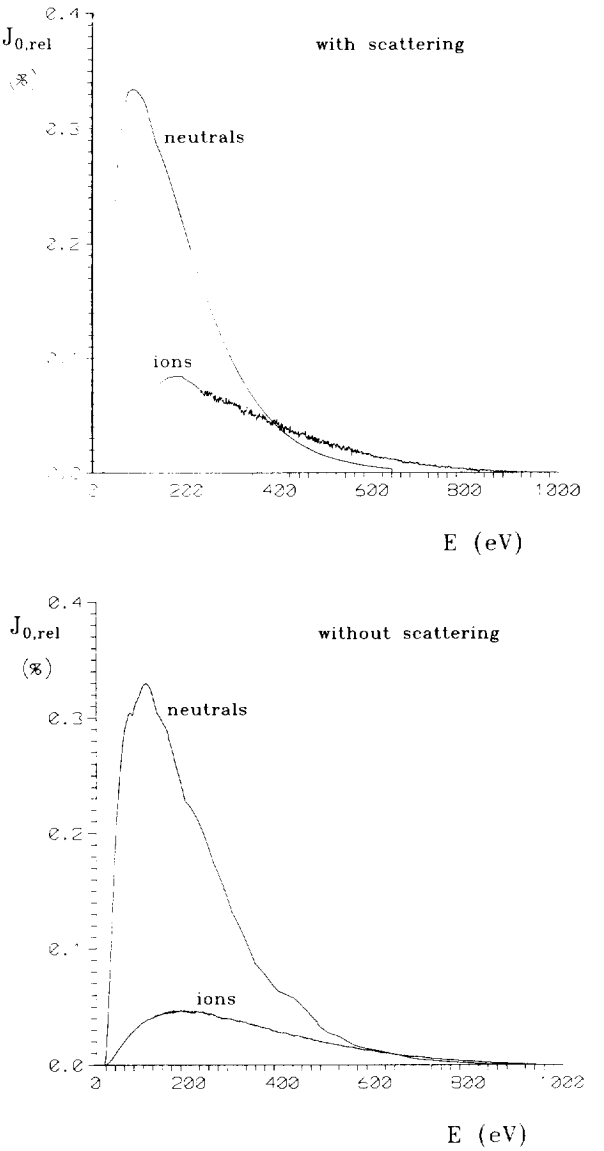

Fig. 12. Relative contribution of the Ar ion and fast neutral bombardment to the sputtering process, calculated with (a) and without (b) scattering.

compared to the case without scattering. The incorporation of scattering has also a slight effect on the atomization process in a glow discharge, since it yields a decrease in sputtering by a factor of 1.5 to 2, and also slightly decreases the contribution of fast atom bombardment compared to ion bombardment to the sputtering process. Our conclusion is that anisotropic scattering and elastic collisions are rather important processes which should not be neglected in modelling of glow discharge systems.

Acknowledgements—A. Bogaerts is indebted to the National Science Foundation (NFWO) for financial support. This research is also sponsored by the Federal Services for Scientific, Technical and Cultural Affairs (DWTC/SSTC) of the Prime Minister's office through IUAP-III (conv.49).

References

[1] B. Chapman, *Glow Discharge Processes*, John Wiley, New York (1980).
[2] R. K. Marcus, *Glow Discharge Spectroscopies*. Plenum Press, New York (1993).
[3] W. W. Harrison, Glow discharge mass spectrometry, in *Inorganic Mass Spectrometry* Eds, F. Adams, R. Gijbels and R. Van Grieken. Wiley, New York (1988), pp. 85–123.

[4] N. Jakubowski, D. Stuewer and W. Vieth, *Fres. Z. Anal. Chem.* **331**, 145 (1988).
[5] F. L. King and W. W. Harrison, *Mass Spectrom. Rev.* **9**, 285 (1990).
[6] W. W. Harrison, K. R. Hess, R. K. Marcus and F. L. King, *Anal. Chem.* **58**, 341A (1986).
[7] W. W. Harrison and B. L. Bentz, *Prog. Anal. Spectrosc.* **11**, 53 (1988).
[8] K. R. Hess and R. K. Marcus, *Spectroscopy* **2**, 1 (1987).
[9] W. W. Harrison, C. M. Barshick, J. A. Klingler, P. H. Ratliff and Y. Mei, *Anal. Chem.* **62**, 943A (1990).
[10] D. B. Graves and K. F. Jensen, *IEEE Trans. on Plasma Science* **14**, 78 (1986).
[11] W. Schmitt, W. E. Köhler and H. Ruder, *J.Appl.Phys.* **71**, 5783 (1992).
[12] M. Meyyappan and J. P. Kreskovsky, *J.Appl.Phys.* **68**, 1506 (1990).
[13] J. P. Boeuf, *J.Appl.Phys.* **63**, 1342 (1988).
[14] J. P. Boeuf, *Phys.Rev.A* **36**, 2782 (1987).
[15] M. Surendra, D. B. Graves and G. M. Jellum, *Phys.Rev.A* **41**, 1112 (1990).
[16] R. J. Carman and A. Maitland, *J.Phys.D* **20**, 1021 (1987).
[17] R. J. Carman, *J.Phys.D* **22**, 55 (1989).
[18] I. Abril, *Comp.Phys.Comm.* **51**, 413 (1988).
[19] J. P. Boeuf and E. Marode, *J.Phys.D* **15**, 2169 (1982).
[20] Tran Ngoc An, E. Marode and P. C. Johnson, *J.Phys.D* **10**, 2317 (1977).
[21] Z. Wronski, *Vacuum* **42**, 635 (1991).
[22] A. C. Dexter, T. Farrell and M. I. Lees, *J.Phys.D* **22**, 413 (1989).
[23] M. J. Kushner, *J.Appl.Phys.* **58**, 4024 (1985).
[24] F. W. Aston, *Proc.Roy.Soc.* **A48**, 526 (1911).
[25] A. Bogaerts, B.Sc.Thesis, University of Antwerp (1993).
[26] J. B. Hasted, *Physics of Atomic Collisions*, Butterworth, London (1972).
[27] J. Sielanko, *Radiat.Eff.Lett.* **86**, 185 (1984).
[28] I. Abril, A. Gras-Marti and J. A. Valles-Abarca, *J.Vac.Sci.Technol.* **A4**, 1773 (1986).
[29] R. S. Robinson, *J.Vac.Sci.Technol.* **16**, 185 (1979).
[30] E. Eggarter, *J.Chem.Phys.* **62**, 833 (1975).
[31] W. C. Fon, K. A. Berrington, P. G. Burke and A. Hibbert, *J.Phys.B* **16**, 307 (1983).
[32] F. J. de Heer, R. H. J. Jansen and W. van der Kaay, *J.Phys.B* **12**, 979 (1979).
[33] M. van Straaten, Ph.D.Thesis, University of Antwerp (1993).
[34] M. van Straaten, R. Gijbels and A. Vertes, *Anal.Chem.* **64**, 1855 (1992).
[35] M. van Straaten and R. Gijbels, Fundamental aspects of an analytical glow discharge, in: *Applications of Plasma Source Mass Spectrometry*, Eds G. Holland and A. N. Eaton. The Royal Society of Chemistry, Cambridge (1993), pp. 130–139.
[36] R. S. Mason, D. M. P. Milton, M. Pichilingi, P. D. J. Anderson and M. T. Fernandez, *Rapid Comm. in Mass Spectrom.* **9**, 187 (1994).
[37] J. A. Valles-Abarca and A. Gras-Marti, *J.Appl.Phys.* **55**, 1370 (1984).
[38] M. van Straaten, A. Vertes and R. Gijbels, *Spectrochim.Acta* **46B**, 283 (1991).